AIAA JOURNAL
Vol. 34, No. 5, May 1996

Turbulent Boundary Layer in an Adverse Pressure Gradient: Effectiveness of Riblets

J. R. Debisschop* and F. T. M. Nieuwstadt†
Delft University of Technology, 2628 AL Delft, The Netherlands

Measurements of skin friction by means of a drag balance and of velocity profiles by means of a hot wire have been carried out in the boundary layer over a flat plate in a wind tunnel. A convergent/divergent test section produces a moderate adverse pressure gradient in the divergent part. The purpose of the present study is to investigate the characteristics of this boundary layer and to examine the effectiveness of riblets for skin-friction reduction. We find that the mean velocity follows a logarithmic profile that is shifted downward with respect to the logarithmic law for a zero-pressure-gradient boundary layer. The profile of the streamwise velocity fluctuations exhibits two maxima. Application of riblets in this case leads to a skin-friction reduction of 13%, which implies a considerable increase over the 6% obtained in the zero-pressure-gradient boundary layer. Measurements with a hot wire show that only close to the wall is the mean velocity affected by the presence of riblets and that streamwise velocity fluctuations are reduced here.

I. Introduction

THE reduction of skin-friction in a turbulent boundary layer has been the subject of many studies, and for a review we refer, for example, to Coustols and Savill.[1] One of the most promising skin-friction reduction techniques appears to be the application of so-called riblets on the surface. Riblets are small wall grooves aligned with the main direction of the flow. It is generally established that with these riblets a skin-friction reduction of about 6% can be obtained in a boundary layer with zero-pressure gradient.

In practical applications, however, most boundary layers are subjected to pressure gradients. For the case that the boundary layer is under influence of, e.g., an adverse pressure gradient, the skin-friction reduction effect of riblets is not as well known. A discussion of some experimental results on the effect of pressure gradient has been presented by Walsh.[2] It appears that for small pressure gradients, the riblets are still effective, and the skin-friction reduction is almost unchanged. For moderate and strong pressure gradients, the opinions diverge, i.e., some authors[3,4] report that riblets loose their effectiveness, whereas others[2,5] report that the effectiveness remains at least unchanged. In a previous study[6] this difference in opinion has been explained as most probably due the fact that in these studies the momentum integral balance is applied to evaluate the skin friction, but it is well known that this method is susceptible to error.

A study from Choi[5] showed that near-wall turbulence in a boundary layer over riblets is not affected by the pressure gradient. This may suggest that the riblets keep their skin-friction reducing ability for an adverse pressure gradient. In the study by Nieuwstadt et al.,[6] some measurements were reported on skin-friction reduction for the case of a weak adverse pressure-gradient boundary layer. The observations were done with a drag balance, which avoids the problems connected to application of the momentum balance method. The measurements show that the effectiveness of riblets even increases somewhat in this case. It is not clear whether this result remains valid in a moderate or strong adverse pressure gradient. Therefore, the purpose of this paper is to extend the results of Nieuwstadt et al.,[6] to a stronger adverse pressure gradient. At the same time, we propose to study the influence of the pressure gradient on the profiles of the mean velocity and of the turbulent velocity fluctuations, both over a smooth and a riblets surface.

Received Dec. 6, 1994; revision received June 5, 1995; accepted for publication June 7, 1995.

*Postdoctoral Researcher, Laboratory for Aero and Hydrodynamics, Rotterdamseweg 145.

†Professor, Laboratory for Aero and Hydrodynamics, Rotterdamseweg 145.

In this study we will consider two types of riblets. These are the standard triangular shape and riblets with a trapezoidal shape. According to Bechert,[7] the latter riblets perform better under zero-pressure gradient where they lead to about 9% skin-friction reduction. Measurement of the skin-friction reduction resulting from the riblets is carried out with the aid of a drag balance. The velocity is measured with a hot wire.

II. Experimental Setup

The experimental setup, which is similar to the one used by Nieuwstadt et al.,[6] is illustrated in Fig. 1. The experiments are conducted in a low-speed recirculating wind tunnel in which the velocity can be adjusted from 0 to 25 ms^{-1}. The test section of the wind tunnel has a length (streamwise direction) of 5.7 m, a width of 0.73 m, and a height of 0.89 m. In this test section a 4-m-long flat plate was mounted at a distance of 0.28 m from the bottom wall. The leading edge of the plate is sharp, and an adjustable flap at the trailing edge prevents any leading-edge separation. On this plate a boundary layer develops, and transition to turbulence is forced by a trip wire located 50 cm downstream from the trailing edge. To generate a pressure gradient, the test section was given a convergent/divergent cross section. The measurements were taken in the divergent part of the contraction, as shown in Fig. 2. The contraction was somewhat stronger than in the case of Nieuwstadt et al.[6] so that a stronger adverse pressure gradient could be obtained.

The skin friction is observed with a drag balance constructed following the design of Hirt and Thomann.[8] The force due to friction on a drag plate of 0.54×0.54 m^2 is measured by observing its streamwise displacement with help of a strain gauge. This plate lies on the top of a carrying element that is slightly larger than the drag plate and that is immersed in a oil reservoir. The carrying element is suspended by wires from a frame (see Fig. 1). Between the carrying element and the oil reservoir is a narrow slit with a sharp edge. The surface tension of the oil in this slit compensates the force due to the pressure gradient. Calibration of the drag balance is performed by attaching to the measuring plate a fine wire from which small known weights are suspended. Special care is taken to minimize the friction in the movement of the wire. A calibration is carried out before and after each experiment. For more details, we refer the reader to Nieuwstadt et al.[6] During this previous study, in which a slightly lower pressure gradient was considered, the authors obtained an accuracy of, typically, 1% with this drag balance.

A pitot tube is located 15 cm above the center of the drag balance. During all of the experiments, to be discussed in the following, the velocity V_0 given by this pitot tube was recorded, and it was later used for the data analysis. Velocity profiles were measured with single hot-wire probe. A fully automatic Quin displacement

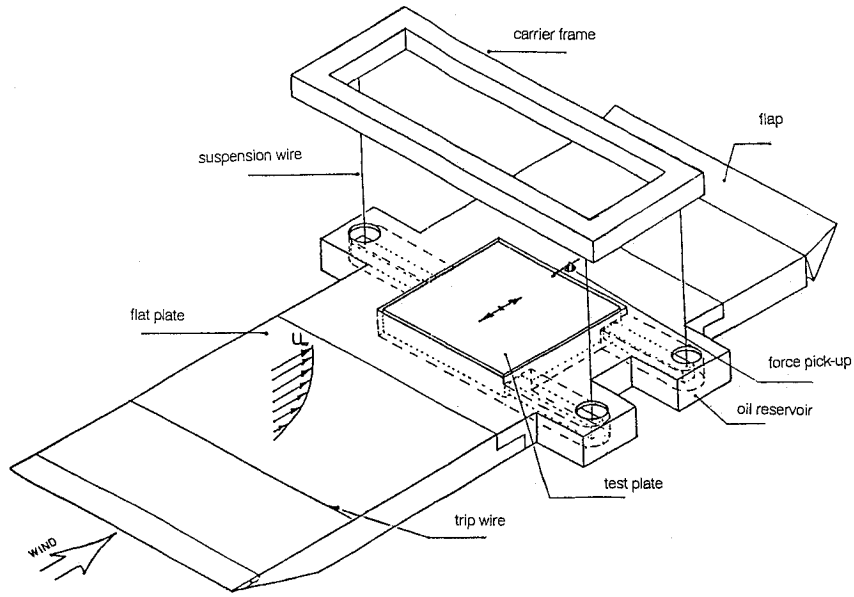

Fig. 1 Experimental setup of the flat plate and the drag balance.

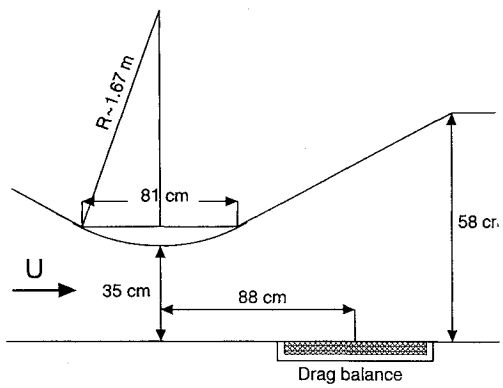

Fig. 2 Description of the wind-tunnel test section.

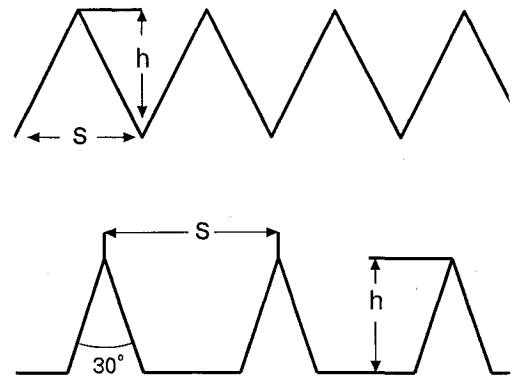

Fig. 3 Description of the riblets shape.

system controlled by a personal computer is used to perform the displacement normal to the wall. This system has a typical accuracy of 0.01 mm for a total displacement of 10 cm. The first position close to the wall is determined by measuring the distance between the probe and its reflection on the wall with the aid of a telescope. The typical error of this measurement is estimated to be 0.05 mm. For the measurements over the riblets surface, the first hot-wire position was determined by measuring the distance between the wire and its shadow with illumination from above. The accuracy, in this case, is estimated to be 0.08 mm. A calibration of the hot wire by means of a fourth-order polynomial is performed before and after each measurement of a velocity profile to correct for possible drift. Each measuring point consist of the acquisition of 10,000 samples at a frequency of 700 Hz with the help of Viewdac data acquisition software. The signal array is converted in a velocity array before calculating statistics, such as the mean value and standard deviation. In this way nonlinearity effects are prevented. The reproducibility of the velocity measurements was found to be better than $\pm 1\%$.

The riblets surfaces are manufactured by machining a PVC pipe on a lathe. During the manufacturing procedure (see also Nieuwstadt et al.[6]) we take a special care of the quality of the riblets (e.g., the sharpness of the tips). Two kinds of riblets shape are selected, as illustrated in Fig. 3. A standard V shape with a height h equal to the width s and a trapezoidal shape with a height over width ratio $h/s = 0.5$. This trapezoidal shape was chosen following a study from Bechert[7] in which a skin-friction reduction of 9% was obtained in a zero adverse pressure-gradient boundary layer. For each of these shapes two sizes of riblets have been used, $s = 0.36$ and 0.64 mm for the V shape and $s = 0.48$ and 0.72 mm for the trapezoidal shape.

III. Results

A. Main Flow Characteristics

The main characteristics of the flow are investigated with a reference velocity $V_0 = 13.5\ \mathrm{ms}^{-1}$. The evolution of the pressure coefficient $C_p = (P - P_0)/\frac{1}{2}\rho V_0^2$ is presented in Fig. 4 together with the evolution of the external mean velocity V_e. The pressure coefficient is calculated from velocity measurements taken 15 cm above the plate outside the boundary layer. P_0 and V_0 correspond to the pressure and the velocity, respectively, above the middle of the drag balance, i.e., at the pitot tube location where the coordinate X is chosen to be 0.

Boundary-layer velocity profiles have been measured at several X locations. From these velocity profiles, we have calculated the characteristic parameters of the boundary layer. These are the displacement thickness δ^* and of the momentum thickness θ, which are shown in Fig. 5. At each X position several profiles have been measured. The results from each of these profiles correspond to a data point in the figure. We find that the reproducibility of the data obtained from different measurements is typically better than 1%.

The evolution of the shape factor $H = \delta^*/\theta$ is plotted in Fig. 6. A monotonic increase is observed until $X = 50$ mm. Farther downstream the shape factor remains constant, which may indicate that the boundary layer has reached equilibrium.[9] This is confirmed by the evolution of the Clauser parameter $\beta = \delta^*/\tau_w\, \mathrm{d}P/\mathrm{d}x$ (the determination of the wall shear stress τ_w will be explained subsequently), which is also plotted in Fig. 6 and which also reaches a constant value after $X = 50$ mm. The values of β vary between 1.8 and 2.4, and this is representative for a moderate adverse pressure gradient, which is, for example, representative for the flow conditions near the trailing edge of an airfoil.

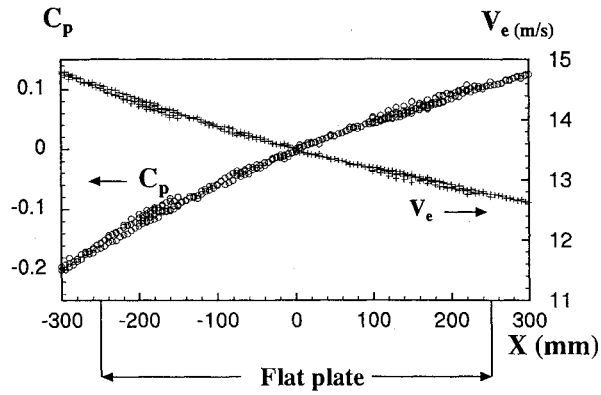

Fig. 4 External velocity and pressure coefficient evolution in the streamwise direction.

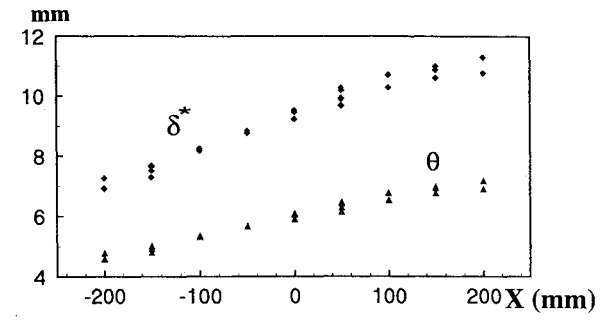

Fig. 5 Downstream evolution of the displacement thickness δ^* and of the momentum thickness θ; each data point gives the result of a single profile measurement.

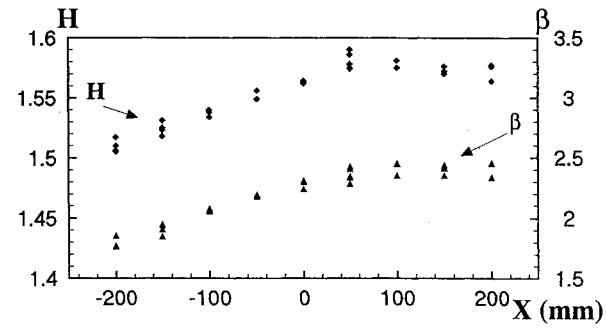

Fig. 6 Downstream evolution of the shape factor $H = \delta^*/\theta$ and of the Clauser parameter $\beta = \delta^*/\tau_w\, dP/dx$.

B. Skin-Friction Measurements

1. Smooth Surface

The measurements by the drag balance are expressed in terms of the friction coefficient C_f that is defined as $C_f = D/\frac{1}{2}\rho V_0^2 A$, where D is the total force on the drag plate, V_0 the reference velocity above the middle of the drag balance, and A the surface of the drag plate. The observations of C_f are plotted in Fig. 7 as a function of the Reynolds number based on the momentum thickness, i.e., $Re_\theta = V_0\theta/\nu$, where: ν is the kinematic viscosity. For the θ we take the observations averaged over the drag plate at a velocity $V_0 = 13.5\,\mathrm{ms}^{-1}$. The variation in Reynolds number is, thus, obtained by varying the wind-tunnel speed. In other words, we neglect the variation of θ. Some estimates show that for the range of Reynolds considered here the variation of θ is less than 3%. Each symbol in Fig. 7 corresponds to a different set of measurements taken at a different day and with a different calibration. Good reproducibility is found between various data sets with a typical variation of $\pm 2\%$.

In Fig. 7 we have also plotted two empirical relations for C_f. These are the well-known expression by Ludwieg and Tillmann,[10]

$$C_f \approx 0.246(V_0\theta/\nu)^{-0.268}10^{-0.678H}$$

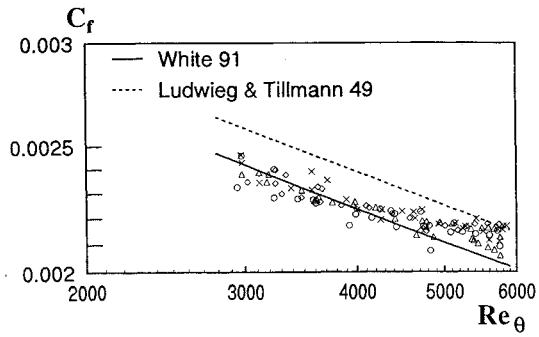

Fig. 7 Skin-friction coefficient measured by the drag balance in comparison with the expression proposed by White[11] and Ludwieg and Tillmann.[10]

and the expression proposed by White,[11]

$$C_f \approx \frac{0.3e^{-1.33H}}{(\log_{10} Re_\theta)^{1.74+0.31H}}$$

Both expressions use the shape factor H and the momentum thickness θ to determine C_f. With the parameters presented in Figs. 5 and 6, we have used these relations to calculate the C_f at the X locations along the drag plate where velocity profiles have been measured. Based on these values, an average C_f of the drag plate is calculated as a function of the Reynolds number based on momentum thickness. As a result, the value given by each formula is consistent with the value obtained experimentally, which is also a spatial average. These are the curves plotted in Fig. 7. Note that to calculate these curves we have varied only the velocity V_0 and the values of θ and H have been kept constant. This may result in some errors, in particular at low values of the Reynolds number (say, Re_θ less than 4500), and this may explain the difference in slope between the experiments and the empirical curves. Nevertheless, it follows from Fig. 7 that our observations of C_f agree within $\pm 2\%$ of scatter with the empirical relationships. However, we note that our experiment was not designed to measure the exact value of the skin friction as function of Reynolds number. Nevertheless, we consider this result to be a confirmation of the fact that our drag balance can measure the C_f without substantial errors due to the pressure gradient.

The expression proposed by White[11] gives a slightly better agreement with the measurements. Thus, we conclude that White's expression is more appropriate for the calculation of the skin friction at values of Reynolds number corresponding to values of this experiment.

2. Riblets Surface

The first results concern the V-shape riblets. The drag plate was adjusted vertically so that the riblets protrude by $0.5h$ above the surrounding flat plate. The skin-friction reduction is expressed as

$$\frac{\partial C_f}{C_{f0}} = \frac{C_f - C_{f0}}{C_{f0}}$$

where C_f denotes the measurement with the drag plate covered with riblets and C_{f0} the measurements with the smooth wall. The results are presented in Fig. 8 as a function of s^+, i.e., the span of the riblets in wall coordinates,

$$s^+ = su_\tau/\nu$$

The lowest values of s^+ are obtained using riblets with $s = 0.36$ mm and the largest s^+ with $s = 0.64$ mm. In the region of $s^+ \sim 10$–11, experimental results are obtained with both riblets sizes. Each symbol plotted in Fig. 8 corresponds to a different measurement run. In total, seven runs were taken on different days, and each of these runs used a separate calibration. A somewhat larger scatter can be observed at the lowest values of s^+ and at the values $s^+ \sim 10$–11 where the results from the two sizes of riblets overlap. This is because these measurements were performed when the wind-tunnel velocity is small (typically less than 8 m/s) at which the sensitivity of the drag balance is somewhat lower. It is important to

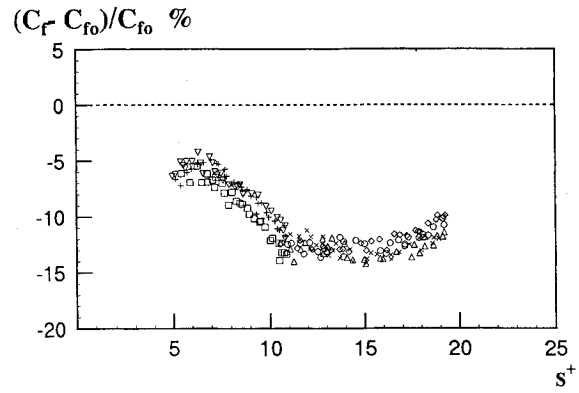

Fig. 8 Relative skin friction obtained with V-shape riblets.

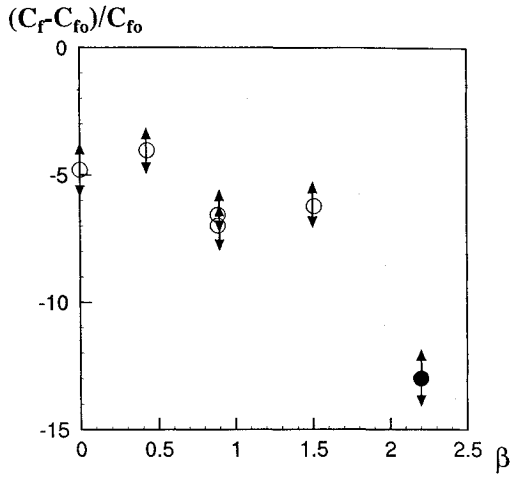

Fig. 9 Evolution of the relative skin friction vs pressure gradient; open symbols: experiments by Nieuwstadt et al.[6]; closed symbol: present study.

note that the results obtained for $s^+ \sim 10$–11 are similar with both size of riblets. This feature gives us confidence in our results and that eventual effects of the pressure gradient on the drag balance are negligible. For each size of riblets, these values of s^+ were obtained with different velocities and, thus, different pressure differences between upstream and downstream the plate. The agreement of the results for the two sizes of riblets tends to deny any pressure influence on the drag balance. The results presented here were obtained with the riblets protruding at half their height. Several tests have been performed to check the influence of the protrusion height on the measurements. No particular behavior could be observed, the results being similar to these presented here.

We find a maximum skin-friction reduction of 13%, which is obtained for s^+ between 10 and 16. This reduction is quite substantial compared to the 5% at zero-pressure gradient, and this follows the trend found by Nieuwstadt et al.,[6] who observed that the drag reduction by riblets increases for adverse pressure gradients. The experimental data of Nieuwstadt et al.[6] together with the present results are illustrated in Fig. 9 where the maximum skin-friction reduction is shown as a function of β. As additional evidence of increased skin-friction reduction for an adverse pressure gradient, we mention the observations of Sundaram et al.[12] who obtained up to 15% skin-friction reduction on the suction side of an airfoil at angle of attack of 6 deg, for which the boundary layer corresponds to a Clauser parameter of 1.06. Note that for an airfoil the effect of the pressure gradient is combined with an effect of curvature, which may explain the somewhat higher percentage of drag reduction than found in our measurements. Because of the dimensions of the flat plate, some streamwise evolution of the skin-friction coefficient can be expected. These evolutions have been carefully investigated. Although they may induce some uncertainty in the determination of s^+, the uncertainty was estimated to be up to 5%. Taking in account the consistency of the measurement procedure and the range of s^+

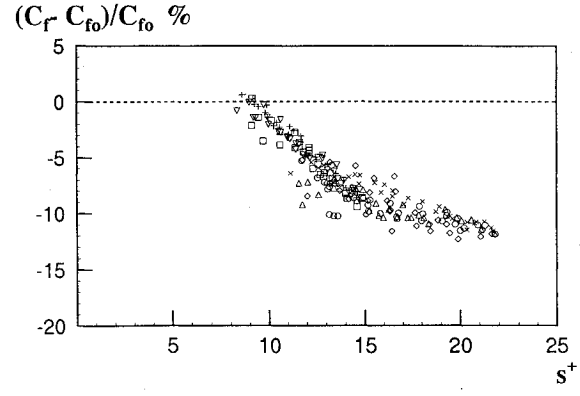

Fig. 10 Relative skin friction obtained with trapezoidal shape riblets.

where the maximum reduction is obtained, we consider that this effect does not affect our results in an important way.

The measurements with the trapezoidal riblets are presented in Fig. 10. The evolution of the skin-friction reduction vs s^+ is different from that found in Fig. 8. A shift of the $\partial C_f/C_{f_0}$ data toward high values of s^+ is observed, and the maximum skin-friction reduction seems to be located at $s^+ > 20$, i.e., outside the range of our riblets sizes. Such a high value of s^+ does not correspond to the value of s^+ for maximum drag reduction at zero-pressure gradient that has been measured by Bechert.[7] It seems that the maximum value of skin-friction reduction is somewhat higher than 12%. In view of the 9% obtained at zero-pressure gradient, the influence of the adverse pressure gradient appears to be, once again, a drastic increase of the riblets effectiveness. Note that the difference of maximum reduction between the V and the trapezoidal shapes is, in this case, a few percent. For zero-pressure gradient, the friction reduction obtained by trapezoidal riblets is almost twice that obtained with standard V shapes (respectively, 9 and 5%). Thus, we conclude that under the influence of a pressure gradient, this difference becomes smaller.

C. Velocity Profile

1. Mean Velocity

Velocity measurements have been carried out both over the smooth and the riblets-covered surfaces. The results presented here have been obtained with the V-shaped riblets. The effect of the riblets on the velocity was found to be similar for the trapezoidal shape. Note that under the influence of a pressure gradient the standard velocity law in the viscous sublayer is affected and the standard linear profile is not appropriate. As a result, the virtual origin of the velocity profile over riblets could not be determined using any analytical approach or experimental results available in the literature. In our case, we assumed that the value of the protrusion height remains close to the value obtained at zero-pressure gradient with the same riblet shape. Therefore, the virtual origin was estimated to be $0.2s$ below the top of the riblets.

The mean velocity profile over a smooth surface and riblets surface is presented in Fig. 11. The profiles are measured above the middle of the drag plate, i.e., $X = 0$. The freestream velocity V_0 is equal to 13.5 ms^{-1}. The nondimensional riblets size at this velocity is $s^+ = 17$. The velocity is normalized by the freestream velocity V_0, and the coordinate y is normalized by the displacement thickness δ^*. To present more detail on the shape of these profiles near the surface, we chose to plot them with a logarithmical y axis. In Fig. 11 the results of several measuring runs have been plotted that fall closely on top of each other.

We note that except for small values of y/δ^*, there is almost no difference between the profiles above the smooth and the riblets wall. In other words, the riblets do not significantly affect the velocity profile. This is confirmed by the values of the momentum thickness, displacement thickness, and shape factor for the two walls, shown in Table 1. The effect of the riblets is only a slight reduction of the velocity close to the wall, i.e., the buffer region of the velocity profile over the riblets wall appears to extend toward higher y values. This leads to a small decrease of the momentum and displacement thicknesses, and as a result, a small increase of the shape factor H.

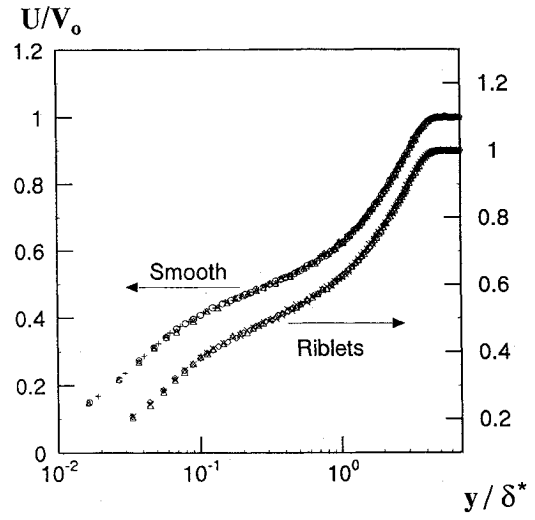

Fig. 11 Velocity profiles in external coordinates U/V_0 and y/δ^*.

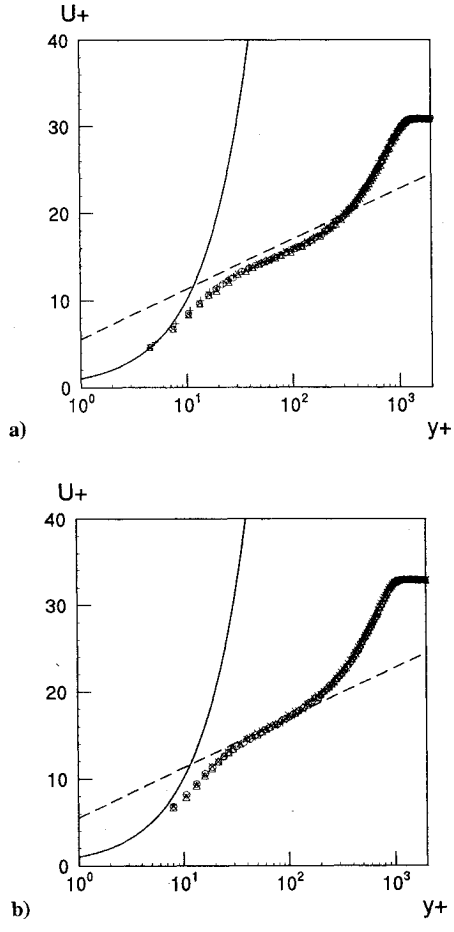

Fig. 12 Velocity profiles in wall coordinates; dashed line $u^+ = 1/\kappa \ell_n y^+ + 5.5$, solid line $u^+ = y^+$: a) smooth and b) riblets.

Complementary information follows when the velocity profiles are plotted in wall units. This has been done in Fig. 12. Figure 12a shows observations over the smooth wall. One may note that this velocity profile falls below the standard logarithmic law $u^+ = 1/\kappa \ell_n y^+ + B$, with $\kappa = 0.4$ and $B = 5.5$ that is representative for the zero-pressure-gradient boundary layer. Nevertheless, a logarithmic profile seems valid between $y^+ = 30$ and $y^+ = 150$ but with a value of B smaller than 5.5. This result agrees well with experiments by Nagano et al.[13] and by Spalart and Watmuff.[14]

For the riblets, the smaller value of u_τ results in an upward displacement of the velocity profile so that the standard logarithmic profile again seems to be followed.

Table 1 Main characteristics of the boundary layer at $X = 0$ for smooth and riblets surface

	Smooth	Riblets
H	1.56	1.57
θ, mm	6	5.75
δ^*, mm	9.33	8.95

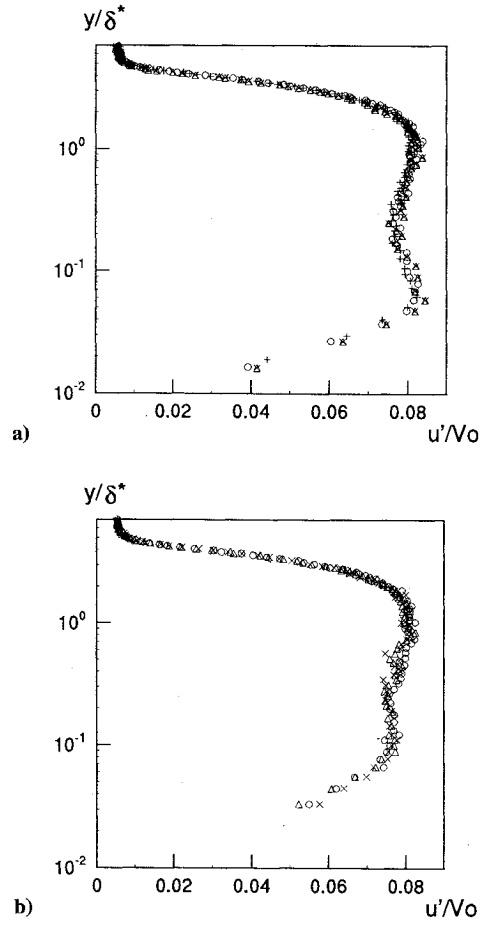

Fig. 13 Profiles of streamwise velocity fluctuations: a) smooth surface and b) riblets surface.

2. Fluctuating Velocity

In Fig. 13 we compare the profiles of streamwise velocity fluctuations obtained above a smooth and a riblets surface. A profile with two peaks is observed. This is characteristic for the adverse pressure-gradient boundary layer. The highest peak, which occurs in the outer part of the boundary layer ($y^+ \simeq 300$), is connected to the strength of the adverse pressure gradient. The smaller peak, close to the wall, corresponds to the level of maximum turbulence production for boundary layers without pressure gradient, i.e., $y^+ \simeq 20$.

In Fig. 13 we show the profiles of the velocity fluctuations nondimensionalized with the free-stream velocity as a function of y/δ^*. Comparison between results for the smooth and riblets surfaces shows that the riblets only affect the fluctuation level close to the surface. In the outer part of the boundary layer, the fluctuations are the same in both cases.

In Fig. 14 we present the same profiles of the streamwise velocity fluctuations but now plotted in wall units. It appears that the peak close to the wall has the same magnitude for both the smooth and riblets surface, i.e., $u'/u_\tau \simeq 2.5$. This confirms our remark, made earlier, that this peak is connected to the turbulence production that directly determines the friction velocity u_τ. In other words, the reduction of the turbulence level near the wall is proportional to the reduction of the friction velocity. This result suggests that observation of the reduction of the turbulence level near the wall

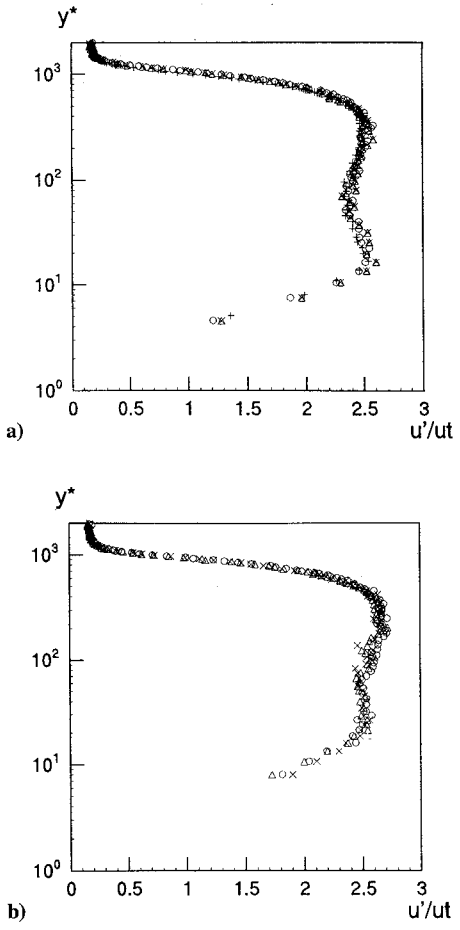

Fig. 14 Profiles of streamwise velocity fluctuations in wall coordinates: a) smooth surface and b) riblets surface.

can be used as an alternative method of measuring the skin-friction reduction by riblets.

IV. Conclusion

With our experimental setup we have been able to generate a turbulent boundary layer under the influence of a moderate adverse pressure gradient. Values of the Clauser parameter β up to 2.4 are obtained. The skin friction in this boundary layer was measured with the help of a drag balance. Because of the special design of this balance, the accuracy of the skin-friction measurement is not influenced by errors due to the pressure gradient. Measurements show quite good reproducibility. Satisfactory agreement was found between our measurements of the skin-friction coefficient and some empirical formulas mentioned in the literature.

Our measurements for the case of a riblets surface show that a skin-friction reduction of 13% is obtained with V-shape riblets. This result is consistent with the trend that the effectiveness of riblets increases for an adverse pressure gradient as follows from previous observations by Nieuwstadt et al.[6] It is also in agreement with a recent study from Sundaram et al.[12]

The velocity profiles measured with a hot wire lead us to conclude that the standard logarithmic velocity law is not valid in an adverse pressure gradient, in accordance with experiments from Nagano et al.[13] and Spalart and Watmuff.[14] In agreement with the results obtained by these authors, our measurements show a downward shift of the velocity profile with respect to the standard logarithmic law valid for the zero-pressure-gradient boundary layer.

The effects of riblets on the mean velocity profile is small when the profile is plotted using outer coordinates. A small reduction of the velocity appears close to the wall, and it corresponds to an extension of the buffer region toward higher values of y. A larger difference appears when wall coordinates are used: the reduction of the wall shear stress velocity by the riblets induces a upward shift of the velocity profile.

Additional information is obtained from the profiles of the streamwise velocity fluctuations. Over the smooth plate, the adverse pressure gradient creates a double-peak in the profile. A first maximum appears close to the wall at $y^+ \simeq 20$, and it corresponds to the usual peak of turbulence production. The second peak is found in the outer part of the boundary layer, and it is related to the adverse pressure gradient. The presence of riblets do not affect this second peak that has the same magnitude both above a smooth and riblets wall when fluctuations are normalized by the freestream velocity. In contrast, the second, near-wall peak is affected by the riblets and a reduction of the turbulent fluctuations is observed. When the turbulence profile is plotted in wall coordinates, the magnitude of the near-wall peak is the same above the smooth and riblets wall. This means that the reduction of turbulence close to the wall is directly proportional to the reduction of the shear stress.

Acknowledgment

The first author was supported by the Human Capital and Mobility project of the European Union No. ERBCHBGCT920022.

References

[1]Coustols, E., and Savill, A. M., "Turbulent Skin-Friction Drag Reduction by Active and Passive Means," *Special Course on Skin-Friction Drag Reduction*, AGARD Rept. 786, 8-1–8-80, Pts. 1 and 2, 1992.

[2]Walsh, M. J., "Riblets," *Viscous Drag Reduction in Boundary Layers*, edited by D. M. Bushnell and J. N. Hefner, Vol. 123, Progress in Astronautics and Aeronautics, AIAA, Washington, DC, 1990, pp. 203–261.

[3]Squire, L. C., and Savill, A. M., "Drag Measurements on Planar Riblets Surfaces at High Subsonic Speeds," *Applied Science Research*, Vol. 46, No. 3, 1989, pp. 229–244.

[4]Truong, T. V., and Pulvin, P., "Influence of Wall Riblets on Diffuser Flow," *Applied Science Research*, Vol. 46, No. 3, 1989, pp. 217–228.

[5]Choi, K. S., "Effects of Longitudinal Pressure Gradients on Turbulent Drag Reduction with Riblets," *Turbulence Control by Passive Means*, edited by E. Coustols, Kluwer Academic, Norwell, MA, 1992, pp. 109–120.

[6]Nieuwstadt, F. T. M., Wolthers, W., Leijdens, H., Krishna Prasad, K., and Schwarz van Manen, A., "The Reduction of Skin-Friction by Riblets Under Influence of Adverse Pressure Gradient," *Experiments in Fluids*, Vol. 15, 1993.

[7]Bechert, D. W., private communication, 1994.

[8]Hirt, F., and Thomann, H., "Measurement of Wall Shear Stress in Turbulent Boundary Layers Subject to Strong Pressure Gradient," *Journal of Fluid Mechanics*, Vol. 171, 1986, pp. 91–108.

[9]Clauser, F., "Turbulent Boundary Layers in Adverse Pressure Gradients," *Journal of the Aeronautical Sciences*, Vol. 21, No. 2, 1954, pp. 91–108.

[10]Ludwieg, H., and Tillmann, W., "Untersuchungen über die Wandschubspannung in turbulenten Reibungsschichten," *Ingenieur Archiv*, Vol. 17, 1949.

[11]White, F. M., *Viscous Fluid Flow*, 2nd ed., McGraw–Hill, New York, 1991.

[12]Sundaram, S., Viswanath, P. R., and Rudrakumar, S., "Studies of Turbulent Drag Reduction Using Riblets on a NACA 0012 Aerofoil," Project Document FA9401, National Aerospace Lab., Bangalore, India, 1994.

[13]Nagano, Y., Tagawa, M., and Tsuji, T., "Effects of Adverse Pressure Gradients on Mean Flow and Turbulence Statistics in a Boundary Layer," Eighth Symposium on Turbulent Shear Flows, 1991.

[14]Spalart, P. R., and Watmuff, J. H., "Experimental and Numerical Study of a Turbulent Boundary Layer with Pressure Gradients," *Journal of Fluid Mechanics*, Vol. 249, 1993.